

A new miniaturized sensor for ultra-fast on-board soot concentration measurements

Abstract

In this article we present a design of a new miniaturized sensor with the capacity to measure exhaust particle concentrations on board vehicles and engines. The sensor is characterized by ultra-fast response time, high sensitivity, and a wide dynamic range. In addition, the physical dimensions of the sensor enable its placement along the exhaust line. The concentration response and temporal performance of a prototype such sensor are discussed and characterized with aerosol laboratory test measurements. The sensor performance was also tested with actual engine exhaust in both chassis and engine dynamometer measurements. These measurements demonstrate that the sensor has the potential to meet and even exceed any requirements around the world in terms of on-board diagnostic (OBD) sensitivity and frequency of monitoring. Further to potential OBD applications, this has the capacity to be used as an engine and combustion diagnostics sensor, for example to detect misfiring, cylinder combustion variability, exhaust gas recirculation flowrate, etc.

Introduction

Meeting stringent particulate matter (PM) and particle number (PN) emission limits for diesel light-duty and heavy-duty vehicles necessitates the use of a diesel particle filter (DPF) in the exhaust line. As a consequence, on board monitoring of the DPF performance is required first to make sure that the DPF operates correctly and, second, to confirm that emission limits are met under real-world operation. The latter is performed by on-board diagnostic (OBD) sensors which make sure that specific OBD threshold limits (OTL) are not exceeded.

Currently three different operation principles are implemented in commercial DPF performance monitoring sensors. The first technique relies on particle deposition and resistance measurement [1, 2]. The particles are deposited onto a collection surface, where electrodes are separated by an electrically insulating material. The deposited conductive particles gradually change the surface conductivity. By measuring the resistance between the electrodes it is possible to assess the amount of soot deposited to the surface, which is then linked to the soot particles in the exhaust line. In principle, this method is based on an integral measurement of particle concentration over a period of time, and requires periodic regeneration of the deposition surface for a new deposition cycle to begin. The frequency of those regenerations is a measure of particle concentration. Therefore, the response time of these sensors is from several seconds to minutes, depending on the particle concentration.

The second family of sensors are the ones measuring the amount of deposited soot into the DPF filter. This can be estimated by either

measuring the pressure difference over the filter or by measuring microwave transmittance through the DPF [3].

The third measurement technique involves electrical particle detection. For this, the charge of particles following combustion can be utilized, such as in the PMTrac sensor [4, 5], where the naturally charged exhaust particles are collected inside the sensor by an electric field and an amplified electric current proportional to the particle concentration is measured.

The electrical methods described above rely on the conductivity of the emitted particles, hence on particle properties. Therefore, electrical detection methods appear to be in need of engine specific calibration to accurately detect PM or PN OTL exceedance. Moreover, the sensitivity of electrical resistance and DPF soot loading estimation sensors is not enough to enable reduction of current OTL levels.

On the other hand, many of the widely-used aerosol measurement instruments rely on the diffusion charging of particles by ions generated in a corona discharge. For the measurement of exhaust gas particle concentrations a simplified electrical instrument based on the diffusion charging was first demonstrated by Ntziachristos et al. [6]. The instrument consisted of a particle charger and a Faraday cup aerosol electrometer. In the years since, that same concept has been used in several rather simple aerosol instruments such as NSAM [7] and DiSCmini [8].

In diffusion charging instruments, the charge acquired by the aerosol during the charging process is not only dependent on the particle number concentration but also on particle size and this has an effect to the instrument response. However, in typical exhaust aerosol of either diesel or gasoline vehicles, the mean particle size typically remains within a narrow size range. Since the particle charging process does not significantly depend on the particle material, this detection method is equally suitable for both conductive soot particles and non-conductive ash particles. Diffusion charger based instruments typically offer good correlation and good signal repeatability for a stable size distribution, which also make them a promising approach as an OBD particle sensor.

In this study, a new miniaturized sensor based on particle diffusion charging is presented, with the potential to be used as an OBD sensor or as a general combustion diagnostics sensor.

Operating principle and sensor design

The new sensor is based on the Pegasor PPS-M [9] sensor design, but in a much more compact form. The unit is now designed so, that the sensor probe, measuring 16 mm in diameter and 40 mm in length, can

be positioned directly into the exhaust line. The necessary electronics are integrated to the sensor head, and a CAN serial bus is provided for the data output. The overall dimensions of the sensor are 190 mm length and 36 mm diameter at the largest point. M18×1.5 thread is provided for the connection to the exhaust line. The sample flow rate of the tested prototype sensor was 3.5 lpm, while the required pressurized air supply was 8 slpm with 1.5 bar overpressure compared to the exhaust line.

A schematic of the cross section of the prototype sensor is presented in Figure 1, showing the key components of the design. The operation of the sensor is based on diffusion charging of the aerosol particles and subsequent charge detection. Like the PPS-M sensor, the new sensor utilizes the escaping current measurement method, where the particles need not be actually collected. The charge detection is realized by measuring the charge that the particles carry away from the electrically floating corona discharge. In order to avoid charger fouling, the corona discharge electrodes are protected by a clean sheath air flow and the ions produced are brought into contact with the sample by a high velocity air stream from the discharge region. The same air stream is used as a pump flow providing the sample flow for the sensor.

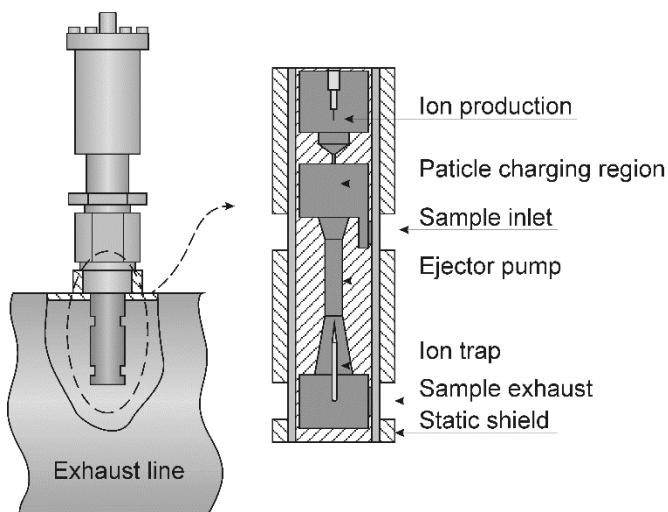


Figure 1. The sensor prototype pictured on the left together with the cross section on the right showing the main components of the sensor design.

The particle charging takes place in the charging region positioned right after the critical orifice separating the discharge region and the sample volume. The sample enters the charging region through the sampling port followed by a sharp bend in the flow channel. The purpose of the bend is to act as a pre-cut impactor preventing the large particles from entering the sensor and clogging the sample flow path. After the charging region the sample flows through the ejector pump. An ion trap is positioned to the ejector pump exhaust to remove the excess ions before the sample exits the sensor through the sample exhaust port. The sample inlet and exhaust ports are positioned on the same side of the sensor probe in order to minimize the pressure difference required from the ejector pump. Although the inlet and exhaust ports are relatively close to each other, the sample recirculation is prevented by the high flow velocity of the exhaust flow.

Sensor response and sensitivity

The sensor output signal is an electrical current produced by the charged particles as they exit the sensor. The sensor response relates this output to the number concentration of the aerosol particles in the

sample flow. The operation is based on diffusion charging of the particles, and hence the response is proportional to the charging efficiency. Since the charging efficiency is dependent on particle size, the sensor response is also a function of it. The charging efficiency depends on the Nit -magnitude, which is the product of the ion number concentration (N_i) and the particle residence time (t) in the charging region. While the charging efficiency could be approximated from the Nit -product, the ion properties, and the particle size, it is however often approximated to follow a power function of the particle size, shown in equation 1. The parameters a and b in equation 1 are typically determined by calibration, where the charger output signal is compared to the aerosol concentration when using monodisperse aerosol in the laboratory.

$$R_s(d_p) = ad_p^b \quad (1)$$

For the prototype sensor it was not possible to produce monodisperse calibration aerosol in sufficient concentrations for the high volumetric flow rate needed for the calibration. Instead, the sensor output was measured with different polydisperse aerosol size distributions as an input. Then, a fitting routine was used in order to find out the parameter values for the charging efficiency. The response measurement setup is shown in Figure 2. The measured test aerosols were produced by a modified diesel fuel burning heater [10]. The size distribution was controlled by varying the fuel feed and the air flow into the burner. The number-weighted geometric median of the size distribution was varied between 35 nm and 210 nm, while the geometric standard deviation range was 1.6 - 1.8. A Scanning Mobility Particle Sizer (SMPS, TSI Inc.), consisting of a model 3071 differential mobility analyzer (DMA, TSI Inc.) and a model 3775 condensation particle counter (CPC, TSI Inc.) was used to measure the size distribution. The total number concentration was measured with a model A20 CPC (Airmodus Oy). In total three ejector dilutors were used for dilution. Two in series, in front of the SMPS, and a third one in series upstream of the CPC. The total dilution ratio for the SMPS measurement was 90:1, and 900:1 for the CPC measurement.

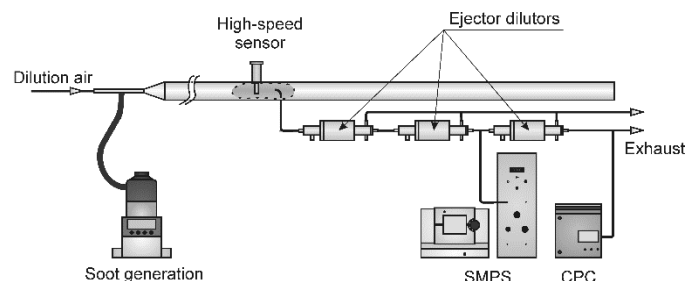


Figure 2. The setup used for the prototype sensor response measurement.

For data processing, the measured total number concentrations were first corrected with the dilution ratio to obtain the total number concentration in the sample line. The measured number size distributions were then normalized to the measured total number concentration of the test aerosol. In order to obtain the values for eq. 1 parameters, the measured sensor signal was compared to a simulated sensor output calculated from the corrected number size distributions using the response function shown in eq. 1. The best fitting values for parameters a and b in the response function were obtained by using a minimum square sum fitting routine. The resulting sensor response is shown in eq. 2 and plotted in Figure 3 together with a correlation plot between the measured and simulated sensor outputs. The measured sensor response points in Figure 3A are plotted as the function of the

median diameter of the size distribution weighted with the sensor response.

$$R_s(d_p) = 0.16d_p^{1.03} \quad (2)$$

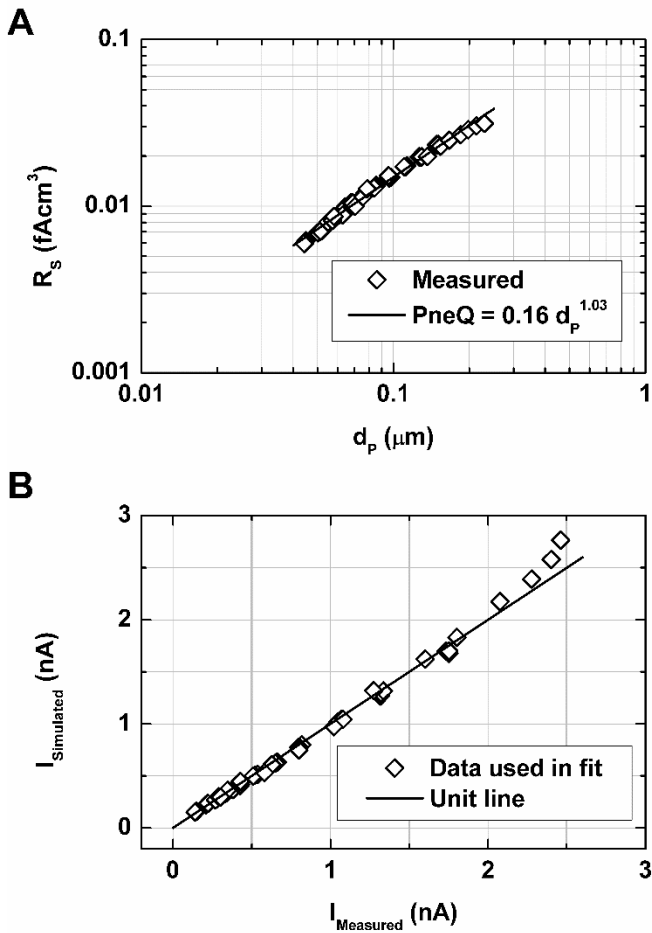


Figure 3. (A) Fitted sensor response as a function of the particle size. The measured response points are plotted as a function of the median size of the size distribution weighted with the fitted response function, and (B) correlation plot between the simulated and measured sensor responses.

The correlation plot in Figure 3B shows a good correlation between the measured and simulated responses, implying that the fitted response adequately describes the sensor behavior in the measured size range. While the overall fit between the response model and the measured data points is very good, it can however be seen that the model starts to slightly deviate from the measurement at the largest particle sizes. In particular, the simulated signal appears to be larger than the measured one. This could be caused for instance by inertial particle losses in the sensor. However, there is relatively high measurement uncertainty in these larger particle sizes, since these approach the SMPS upper size limit. The fitted response however fits rather well in the size range from 40 – 200 nm, which is relevant for typical exhaust particles. The fitted power of 1.03 is in line with corresponding values reported for other electrical aerosol instruments, where diffusion charging is the major charging mechanism [11].

For converting the measured sensor signal to a number or mass emission, an approximation of the size distribution is required. This approximation may vary depending on the application or it may even

be possible to utilize engine operation condition dependent conversion factors, if the engine behavior is known well enough. The needed conversion factors to number and mass emission can be obtained with the help of equations 3 and 4 respectively. In the equations $N(d_p)$ is the approximated size distribution and $\rho(d_p)$ is the density profile of the particles.

$$C_N = \frac{\int N(d_p)R(d_p)dd_p}{\int N(d_p)dd_p} \quad (3)$$

$$C_M = \frac{\int N(d_p)R(d_p)dd_p}{\int N(d_p)\frac{4}{3}\pi d_p^3 \rho(d_p)dd_p} \quad (4)$$

According to the response model for a size distribution, with a count median size of 50 nm and a geometric standard deviation 1.7, the PN detection limit of the prototype sensor is approximately 10^4 $1/\text{cm}^3$, with a sampling interval of 1 s. In terms of raw exhaust conditions, for a passenger car producing exhaust volume in the order of $1 \text{ Nm}^3/\text{km}$, the sensor is able to detect concentrations down to 10^{10} part./km, i.e. more than one order of magnitude lower than current PN emission limits of 6×10^{11} part./km. In terms of mass, and assuming a typical lognormal size distribution as before and a particle density profile for diesel vehicles [12], this would correspond to a soot mass of less than $3 \mu\text{g}/\text{km}$, i.e. several times lower than any PM limits around the world.

Temporal resolution

As already mentioned, the diffusion charging process is dependent on the Nit -product. Unipolar diffusion chargers are typically designed so that the particles reach saturation charge level. According to Davison et al. [13] this is accomplished at Nit -product values above 10^7 s/cm^3 . In the sensor design the ion current produced by the corona and entering the charging region is in the order of hundred nano-amperes, which would correspond to an ion production rate in the order of 10^{12} ion/s. If the ions lifetime is assumed to be 1 ms, and the charging region volume is approximately 0.5 cm^3 , the ion concentration would be above 10^9 ion/ cm^3 . These numbers suggest, that the saturation charge level for the particles would be reached within 10 ms. Another factor affecting the temporal resolution is the gas exchange rate in the sensor. The total sample volume inside the prototype sensor is approximately 1.0 cm^3 . The flow rate inside the sensor sample volume is a sum of the sample flow rate 3.5 lpm and pump flow rate 1 lpm, which equals 4.5 lpm in total. Combining the sample volume and the flow rate leads to a sample residence time of 13 ms inside the sensor, which sets a theoretical lower limit for the response time.

In practice, the electronic noise of the high sensitivity electrometer sets also limitations for the sensor time resolution. The higher the sampling rate and the shorter the integration time the more noise is present in the measured current signal and a higher signal is required for the measurement. To overcome this problem, the integration time of the sensor electrometer can be selected according to the measurement needs. With the highest sampling rate of 100 Hz, the noise level is approximately 1 pA, and with 1 Hz sample rate the noise level drops down to 100 fA.

The temporal performance of the sensor was tested with laboratory measurements using the calibration measurement setup. A step response in the sample concentration was induced by directing a high velocity particle free air stream directly into the sampling port of the sensor. The airstream was controlled by a fast acting magnetic valve

and the flow velocity was adjusted high enough in order to achieve a rapid change in the sample concentration. The sensor output was recorded with 100 Hz sampling frequency and the status information from the magnetic valve was recorded with 800 Hz sample rate. In the data processing the measured step responses were aligned together using the measured valve status signal. Approximately 100 repetitions were averaged to form an average step response, shown in Figure 4A together with a fitted step response. A time constant τ value of 18 ms, gave the best fit to the measured data, which corresponds to a value of 40 ms for a 10 - 90% rise time. The impulse response fit, shown in Figure 4B, was composed from the measured step response data and the fitted step response.

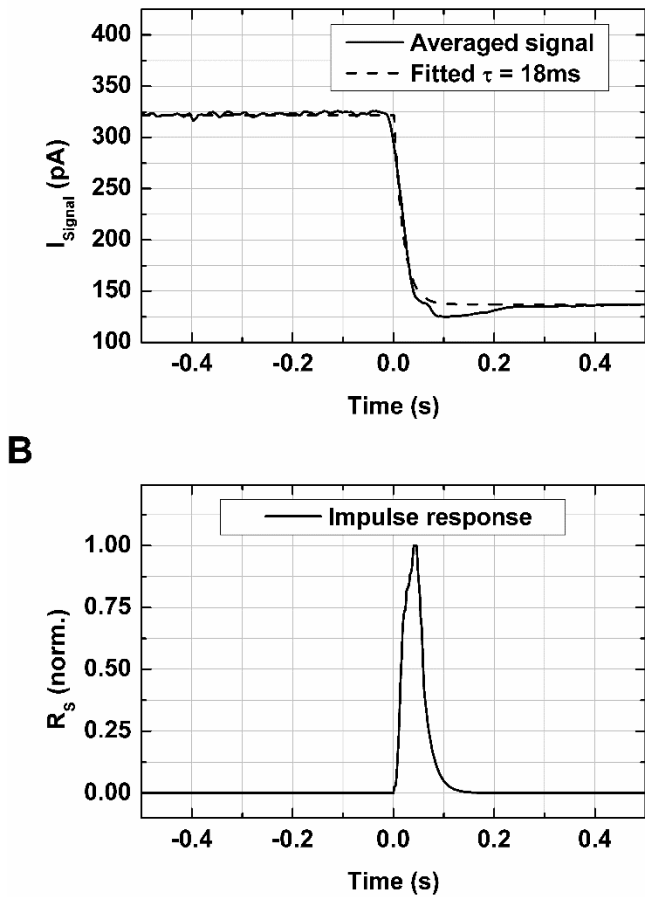


Figure 4. (A) Step response of the prototype sensor as an average of 100 repetitions of rapid concentration drop; a fitted step response with a time constant of 18 ms shown for reference. (B) Fitted impulse response of the prototype sensor.

Performance with real exhaust aerosol

In order to test its performance in real exhaust aerosol, the prototype sensor was fitted at the tailpipe of a light duty vehicle. This mounting point does not represent the targeted mounting point of the sensor in actual applications, but was chosen for practical reasons. The tailpipe was connected to a transfer line leading the exhaust to a Constant Volume Sampler. This guaranteed no backflow of ambient air in the tailpipe. Total particle number concentration measurement was realized with a CPC (Model 3776, TSI Inc., with 2.5 nm cut point) measuring diluted exhaust sample. The dilution system used consisted

of a perforated tube diluter as the first stage dilution, with dilution ratio of approximately 12:1, and an ejector diluter as the secondary dilution stage. The CPC sample was further diluted with a dilution ratio of 42:1. The tested vehicle was Volkswagen Polo 1.2 TSI, equipped with a stoichiometric gasoline direct injection (GDI) engine. The test cycle was the NEDC (New European Driving Cycle), starting with a pre-warmed engine. In the measurement results, shown in Figure 5, the measured raw signal from the sensor and the total number concentration of particles larger than 3 nm are plotted over the test cycle. In the measurement an averaging time of 1 s was used for the prototype sensor signal to match the CPC time resolution. A correlation plot of the signals is shown in Figure 6.

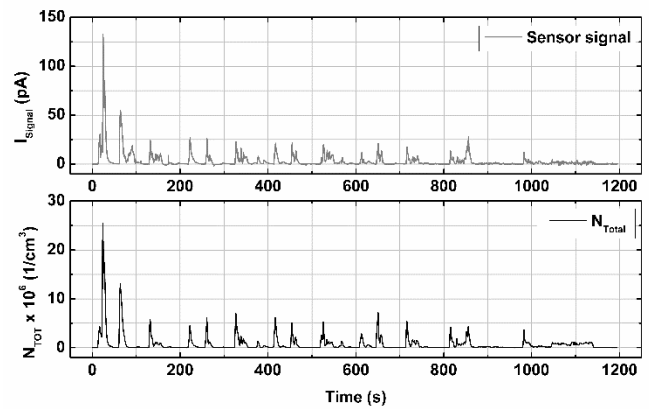


Figure 5. Sensor signal and particle total number concentration measured over the NEDC.

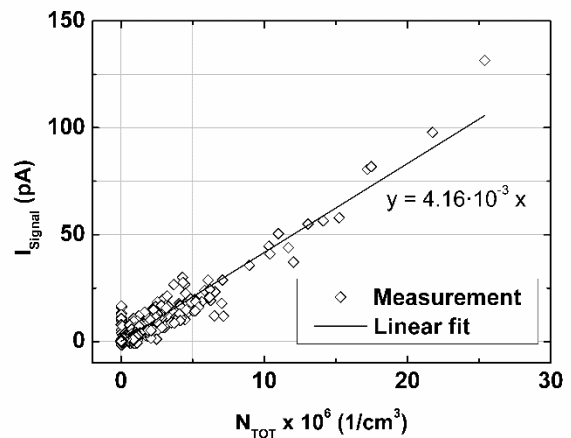


Figure 6. Second-by-second sensor signal and total particle number correlation over the NEDC.

As it can be seen from Figures 5 and 6, the sensor output signal correlates very well to the measured total particle number concentration. The largest difference between the signals is seen in the beginning of the cycle during a period of 75 to 100 s. At this point there is a distinct signal seen from the sensor, while the measured total number concentration was essentially zero. The same difference was observed also in other repetitions; however, the sensor signal amplitude during this time frame varied between the runs. At this point in the NEDC test cycle there is a deceleration from 32 km/h. Since the sensor was mounted at the end of the tailpipe, where the exhaust gas

temperature is much lower than for what the sensor is designed for, it is possible that this behavior is caused by water condensation on the electrical insulators, thus causing an artifact measurement, before it evaporates again.

Application to combustion diagnostics

The fast response characteristics of the sensor prototype were also tested in the engine dynamometer measurements with a six-cylinder, 1000 kW medium speed diesel engine used in locomotives. The sensor was fitted in the exhaust gas recirculation (EGR) line for practical reasons, and the EGR valve position was adjusted so that the concentration measured by the sensor was within the measurement range. Since the EGR line is positioned before the turbocharger the sensor was operating in an elevated exhaust line pressure, reaching 3 bar overpressure and over 500 °C temperature at maximum load point. The sensor air supply pressure was kept 1.5 bar above the exhaust manifold pressure to ensure proper operation of the integrated ejector pump. The outer part of the sensor was cooled with pressurized air, to prevent excessive heating of the electronics.

The in-cylinder pressure was measured from one cylinder in order to have reference engine timing information for the data alignment. The pressure signal was measured at 800 Hz sample rate, while the sensor output was recorded at 100 Hz sample rate. During data processing several time frames containing data from 20 engine revolutions were aligned together with the help of the timing signal. The signals acquired in different frames were then averaged. An example of the measured signal from an engine load point of 750 RPM and 513 kW is shown in Figure 7. The same figure also shows the measured signal at the same load point with the sensor charger switched off. This was recorded in order to test whether the pressure pulses, the high temperature or the charge produced by combustion would disturb the measurement. As seen from the figure, the signal level in the charger-off measurement is close to zero, indicating that the impact of external disturbances to measured values is low.

The signals are plotted as the function of engine crank angle, showing a time span of ten engine revolutions. A clearly repeating waveform is seen with six distinct particle concentration peaks every two engine revolutions. The peak nearest to the 0° crank angle is significantly lower than the others, which may be resulting for instance from the distance between this particular cylinder and the sampling point or the pressure waves inside the EGR line. What is most important in this stage is not to explain the engine particularities but to demonstrate the repeatability and resolution of the sensor in detecting individual combustion events and the related exhaust pulses.

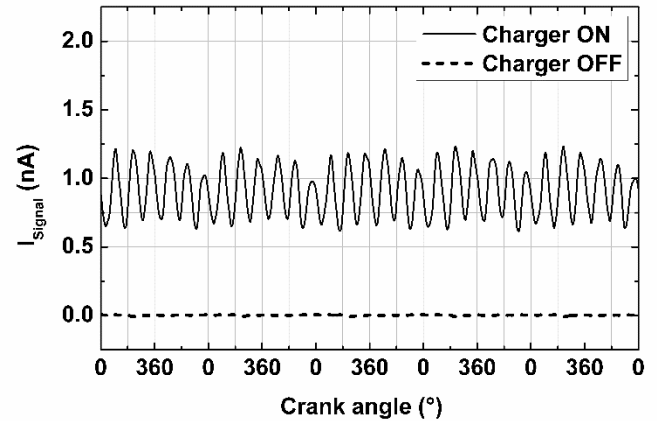


Figure 7. Measured prototype sensor signal (Charger on) from load point 750 RPM/513 kW. Shown also for reference the measured with the sensor charger off at the same load point.

In order to test the sensor's ability to distinguish particle emissions from different cylinders, the fuel injection was delayed in one of the cylinders when the engine was run at the lowest load point of 350 RPM/62 kW. The measurement results are shown in Figure 8. A clear change in the measured signal waveform can be seen indicating higher particle emissions from the delayed injection cylinder due to the poor burning of the fuel. Moreover, different particle exhaust levels for the subsequent combustion cylinders, compared to the reference levels, are observed as the engine is adjusted to match the same output power as in the reference case.

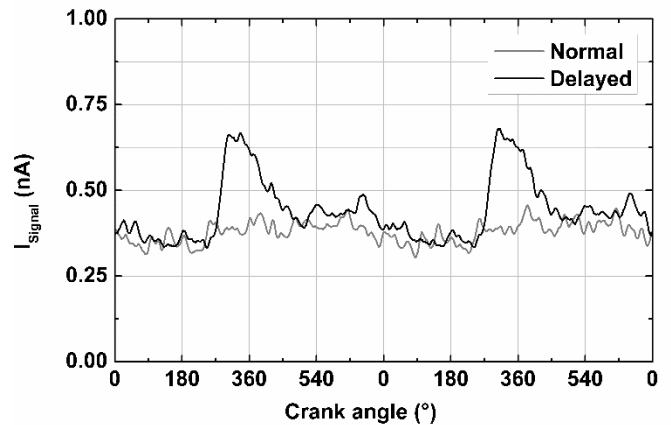


Figure 8. Measured signals from both normal engine operation and delayed fuel injection in one cylinder during load point 350 RPM/62 kW.

Conclusions

The design of a new particle sensor prototype was presented. The sensor is based on diffusion charging and electrical detection of exhaust particles and is intended for on board measurement of soot emissions from engines and vehicles. The study determined the sensor sensitivity and its response to exhaust particles and presented measurement results in real exhaust aerosol.

A fit for the sensor response was obtained from laboratory tests. The obtained response with particle size roughly scales with a power of one and this brings it in good agreement with other diffusion charging based instruments. Using pulse signals, a response time of 18 ms was determined, which is in the same range of the theoretical value estimated from the sensor dimensions and operation principle. Moreover, its sensitivity in terms of PN and PM emissions of passenger cars is in the order of 10^{10} part./km and $3 \mu\text{g}/\text{km}$, respectively. Such performance is by far better than the characteristics of currently used OBD sensors for DPF monitoring.

The sensor performance was validated with transient vehicle chassis tests and steady-state engine dynamometer measurements. A very good correlation between the sensor signal and the measured total number concentration was observed on the chassis dynamometer measurements. Tests on the engine operating at low speed demonstrated that the sensor was able to distinguish particle emission peaks originating from individual combustion events in the different engine cylinders. This demonstrates the potential of the sensor to even be used as a combustion diagnostic.

The prototype sensor requires still further development for practical OBD applications. For instance, the consumption of the pressurized air is a major concern, and one key issue is the minimization of both required pump and sheath air flows. Furthermore, the current prototype is dimensioned for 1.5 bar overpressure, which is quite high but can be decreased. Additionally, the sensor real world performance needs more studying together with other issues like the water condensation in cold conditions, long term operation capability and stability. Although the list of open issues is rather long, the presented approach seems promising for an on board particle emission sensor.

References

1. Hauser, G., (2006) Smoke Particulate Sensors for OBD and High Precision Measuring, SAE Technical Paper 2006-01-3549.
2. Ochs, T., Schittenhelm, H., Genssle, A., and Kamp, B., "Particulate Matter Sensor for On Board Diagnostics (OBD) of Diesel Particulate Filters (DPF)," SAE Int. J. Fuels Lubr. 3(1):61-69, 2010, doi:10.4271/2010-01-0307.
3. Fischerauer, G., Förster, M. and Moos, R. (2010) Sensing the soot load in automotive diesel particulate filters by microwave methods, Meas. Sci. Technol. 21 (2010) 035108.
4. Steppan, J., Henderson, B., Johnson, K., Yusuf Khan, M., Diller, T., Hall, M., Lourdhusamy, A., Allmendinger, K. and Matthews, R. D. (2011). "Comparison of an On-Board, Real-Time Electronic PM Sensor with Laboratory Instruments Using a 2009 Heavy-Duty Diesel Vehicle," SAE Technical Paper 2011-01-0627, doi:10.4271/2011-01-0627.
5. Bilby, D, Kubinski, D, J., Maricq, M. M. (2016) Current amplification in an electrostatic trap by soot dendrite growth and fragmentation: Application to soot sensors. J. Aerosol Sci. 98:41-58, doi: 10.1016/j.jaerosci.2016.03.003.
6. Ntziachristos, L., Giechaskiel, B., Ristimäki, J. and Keskinen, J. (2004) Use of a corona charger for the characterisation of automotive exhaust aerosol, Journal of Aerosol Science, 35 (8), pp. 943-963, doi: 10.1016/j.jaerosci.2004.02.005.
7. Fissan, H., Neumann, S., Trampe, A., Pui, D., and Shin, W. (2007). Rationale and Principle of an Instrument Measuring Lung Deposited Nanoparticle Surface Area. J. Nanopart. Res., 9:53–59, doi:10.1007/s11051-006-9156-8.
8. Fierz, M., Houle, C., Steigmeier, P., and Burtscher, H. (2011). Design, Calibration, and Field Performance of a Miniature Diffusion Size Classifier. Aerosol Sci. Technol., 45(1):1–10, doi: 10.1080/02786826.2010.516283
9. Ntziachristos, L., Fragkiadoulakis, P., Samaras, Z, Janka, K., and Tikkanen, J. (2011). Exhaust Particle Sensor for OBD Application, SAE Technical Paper 2011-01-0626, doi: 10.4271/2011-01-0626.
10. Högström, R., Karjalainen, P. Yli-Ojanperä J., Rostedt, A., Heinonen, M., Mäkelä, J. M., and Keskinen, J. (2012) Study of the PM Gas-Phase Filter Artifact Using a Setup for Mixing Diesel-Like Soot and Hydrocarbons, Aerosol Sci. Technol., 46:9, 1045-1052, doi: 10.1080/02786826.2012.689118
11. Kulkarni, P., Baron, P.A. and Willeke, K. (2011) Introduction to aerosol characterization, in Aerosol measurement: principles, techniques, and applications, edited by Baron, P.A., Kulkarni, P., and Willeke, K. John Wiley & Sons, Hoboken, N.J. 3-13, doi: 10.1002/9781118001684.
12. Maricq, M.M., & Xu, N. (2004). The effective density and fractal dimension of soot particles from premixed flames and motor vehicle exhaust. Journal of Aerosol Science, 35, 1251-1274.
13. Davison, S. W., Hwang, S. Y., Wang, J., and Gentry, J. W. (1985) Unipolar Charging of Ultrafine Particles by Diffusion of Ions: Theory and Experiment. Langmuir 1985:1, 150-158, doi: 10.1021/la00061a027

